Characterization of Ionization Phenomena in Soils Under Fast Impulses

N. Mohamad Nor, A. Haddad, and H. Griffiths

***Abstract*—Protective devices such as spark gaps and surge arresters are used to divert surges to earth. It is, therefore, necessary that earthing systems are designed with a low-magnitude earth impedance value so that the overvoltage protection devices can divert high fault currents effectively to earth for all types of fault. Power frequency characterization of earthing systems is extensively researched and fairly well understood. However, the behavior of such systems under transient conditions is still not fully clarified.**

This paper addresses some of these shortfalls. Laboratory experiments were set up to study the characteristics of the ionization phenomenon in various soil conditions. The soil ionization characteristics were investigated using a proposed new concept of pre- and post-ionization resistances. A measurement technique was developed to establish more accurate estimates of ionization electric field threshold, and an equivalent circuit representation is proposed.

***Index Terms*—Earth resistance, equivalent circuit, impulse tests, soil ionization, threshold electric field, transient response.**

I. Introduction

EXTENSIVE research investigations have led to the basis of many standards that deal with earthing systems, among which are BS 7430:1998 [1], ANSI/IEEE Std 81:1983 [2], IEEE Std 142:1991 [3], and IEEE Std 80-2000 [4]. It is now well accepted that highly nonlinear soil behavior is exhibited by earthing systems under high discharge currents [5]–[11].

It has been suggested that this nonlinear process is due to two main electrical conduction processes: a) thermal effects due to high current magnitudes and b) soil ionization due to field enhancement in trapped air voids inside the soil. Many research studies [12], [13] have been made in relation to the soil discharge processes that take place when the earth electrode is subjected to high impulse current magnitudes. However, to date, these processes are still not well understood.

The development of better equivalent circuit models for earthing systems requires evaluation of thresholds and factors affecting the nonlinear soil behavior. From previous studies [6]–[11], values of threshold electric field (E_c), at which the nonlinear behavior starts to occur, ranging from 1.3 to 20 kV/cm have been reported. These values are not from direct measurements of electric field but were derived from the applied voltage, and their validity is not always justified, especially the high values approaching 20 kV/cm. A number of equivalent circuit representations have also been presented by previous researchers [6], [7]. These revealed that the equivalent circuit representation of earthing systems needs to include the impulse behavior and soil ionization effects.

In this paper, a purpose-built laboratory hemispherical test rig is described. A fast impulse current generator was used to investigate the soil characteristics under high-magnitude surges. The ionization process was investigated in a unique and controlled way so that it was possible for the first time to establish the onset very accurately and quantify the net effect of ionization on the electrode resistance. Using these test results, the threshold critical electric field E_c around the electrode was also determined. The nonlinear soil behavior under high-magnitude current was explained on the basis of the thermal and ionization processes in the soil. Based on this new data, an equivalent circuit representation was also suggested and implemented.

II. Experimental Arrangement

A. Test Set-Up

The double exponential test circuit (see Fig. 1) used in this investigation is capable of generating high voltages up to 50 kV and high current impulses up to 5 kA. The impulse source was configured as a current generator by paralleling three low-inductance, 0.15 μF capacitors rated at 65 kV. The capacitor bank was connected to the dc charging unit with an output of up to 55 kV and switched via an SF_6 spark gap. A tail resistor of 21 kΩ and a front resistor of 50 Ω were adopted in this test circuit in order to obtain impulse shapes with the required front and tail times and also to limit short circuit current magnitudes at breakdown. Current measurement was achieved with a commercially available current transformer of sensitivity 0.1 VA^{-1} and a response time of 20 ns. A D-Dot probe system [15] with a ratio of 10 300:1 and a response time of 40 ns was used for voltage measurements.

The voltage and current signals were captured on a Lecroy 9350 A, 500 MHz Digital Storage Oscilloscope (DSO), and Labview software was utilized for data acquisition and analysis.

B. Test Cell Characteristics

It was found from the reviewed literature that hemispherical test cells have been widely adopted during laboratory tests [8], [9], [17], [18]. This type of geometry may also provide a comparable configuration to earthing systems used at some field sites. In this study, a test cell consisting of a hemispherical container of 47.5 cm diameter was adopted (see Fig. 2). Four connection points were fixed uniformly around the circumference of

Manuscript received August 13, 2004; revised October 17, 2004. Paper no. TPWRD-00368-2004.

N. M. Nor was with the Cardiff University, Cardiff CF24 3AA, U.K., and is now with the Faculty of Engineering, Multimedia University, Malaysia.

A. Haddad and H. Griffiths are with the High Voltage Energy Systems Group, School of Engineering, Cardiff University, Cardiff CF24 3AA, U.K.

Digital Object Identifier 10.1109/TPWRD.2005.852352

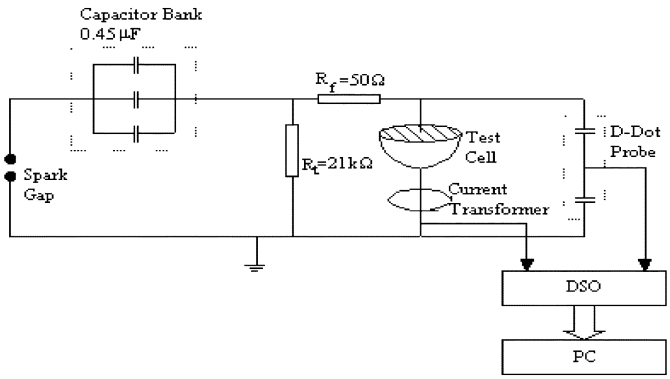

Fig. 1. Impulse current test circuit.

Fig. 2. Hemispherical test cell.

the container to ensure uniform current distribution. A hemispherical electrode (energised electrode) of 6.25 cm diameter was used and was placed in the middle of the container but only half buried inside the sand. This is to avoid excessive electric field magnitudes at the interface between the sand and air and to simulate a hemispherical earth electrode system.

Given the hemispherical configuration, the electric field at a radius r, with $r_1 < r < r_2$, $E(r)$ can be determined from

$$E(r) = \frac{V}{r^2\left(\frac{1}{r_1} - \frac{1}{r_2}\right)} \tag{1}$$

where r_1 = radius of the energised electrode, r_2 = radius of the hemispherical container, and V is the applied voltage at the energized electrode.

C. Soil Medium Preparation

Medium grain size sand of 0.06–0.6 mm is used in these experiments. Sand is chosen since it is easily wetted and dried without loss of physical properties. A sand mixer was used to ensure uniform wetting of the sand. An oven was utilized for drying the sand prior to subsequent experiments. The sand was then poured into the test container and compressed. The sand was compacted manually to avoid sharp edges that may result in air discharges. However, no controlled compaction was made in this study. The energized electrode was half buried inside the sand. Sand with water contents of 1%, 3%, 5%, 7%, 10%, and 15% were used.

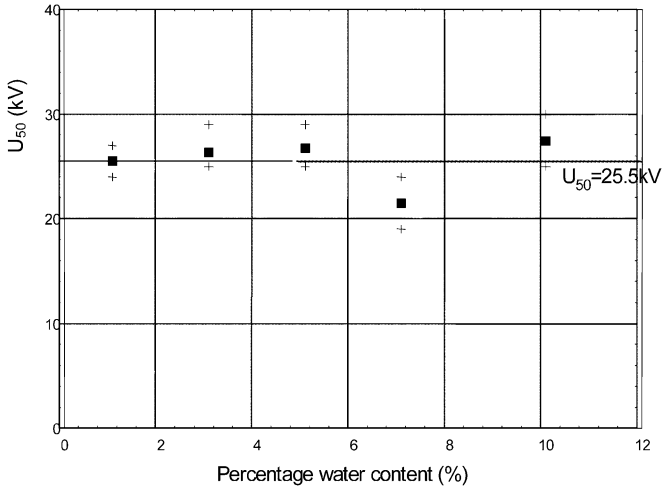

Fig. 3. Breakdown voltage U_{50} for the test cell filled with sand of various water contents.

Furthermore, a salt solution with controlled conductivity was used for calibration of the test system.

D. Test Cell Breakdown Voltage Levels

In order to determine the range of voltage and current magnitudes that could be used during the tests for this adopted configuration, the breakdown voltage of the test cell was measured for various water contents of the sand. The atmospheric pressure, temperature, and humidity in the high-voltage laboratory changed very little during the tests on all samples. Hence, they were considered constant. The up-and-down method, based on IEC60-1:1989 [14] and IEEE-Std 4-1995 [19], was used to determine U_{50} for all samples of wet sands. At least 20 shots were applied for each test sample. The measured values of U_{50} for various sand conditions are shown in Fig. 3. It can be seen that there is a weak influence of water content (resistivity of sand medium) on the U_{50} voltage level. The average value of U_{50} obtained from these tests is 25.5 kV, corresponding to an electric field of 9.4 kV/cm at the energized electrode surface.

III. Calibration Impulse Tests Using a Resistive Liquid Medium

Using the same hemispherical configuration and the test set-up described above, impulse tests were conducted on a resistive salt water solution having a conductivity of 0.7 mS/cm. The purpose of this test was to relate the response of a resistive medium, which was assumed to have a "linear behavior" for all current magnitudes, to wet sand which was found to have nonlinear behavior when subjected to high-magnitude impulse currents. A solution volume of 0.025 m^3 was used to fill the hemispherical container, and the energized electrode was submerged in this resistive solution. Impulse tests were then conducted with increasing current magnitudes. It was observed that the measured impulse voltage had a faster rise time than the current impulse (see Fig. 4), and the current rise time was found to increase with current amplitude. These observations can be explained by the inductive effects of the test circuit components

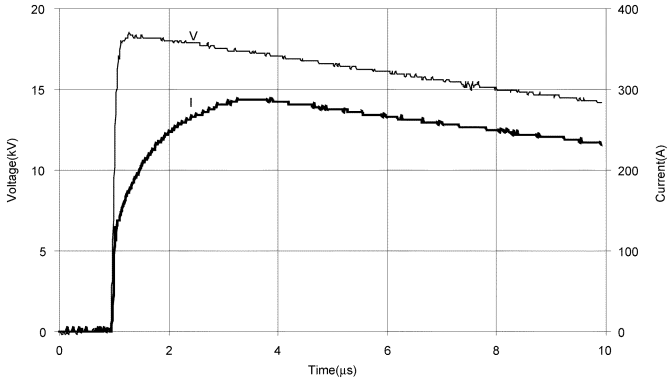

Fig. 4. Typical voltage and current traces for a resistive solution inside the hemispherical container (charging voltage of 20 kV).

and possibly nonlinear thermal and ionic conduction in the resistive liquid.

The measurements showed that the resistance value (measured as the ratio $V_{\text{at Ipeak}}/I_{\text{peak}}$) was nearly constant at 57 Ω for different current magnitudes, and this observation is in agreement with previous investigators [8], [11], [17], [18]. Using this constant resistance value, the conductivity of the resistive solution is calculated

$$R = \frac{\rho}{2\pi}\left(\frac{1}{r_1} - \frac{1}{r_2}\right). \tag{2}$$

From (2) and the value of 57 Ω of R, we obtain $\sigma = 0.78$ mS/cm, which is found to be within 10% of the measured value of 0.7 mS/cm using the conductivity meter.

The achieved accuracy with this resistive load gives a high degree of confidence in the test and measurement set-up adopted in this research program. In this paper, the applied voltage was limited to 35 kV. At higher applied voltages, flashover between the energized electrode and the outer perimeter of the hemispherical container occurred.

IV. Investigations of Soil Ionization Under Impulse Conditions

When impulse tests were conducted on dry sand, the current magnitude was so small that no output signal could be measured. This is due to small conduction current magnitudes in dry soil (high resistivity and large equivalent resistance of test cell), which could not be detected by the transducers adopted in this test program. Again, at applied voltages above 35 kV, flashover between the electrode and outer perimeter of the container occurred.

Impulse tests were also conducted on wet medium-grain sand with different current magnitudes in order to determine the effect of soil ionization process under high-impulse currents.

For the purpose of a better understanding of soil behavior under high-impulse currents, the results are discussed according to current impulse shape and impulse resistance of the test object.

A. Current Impulse Shape Observations

Fig. 5(a) and (b) show the voltage and current traces obtained with tests on wet sand when subjected to an applied voltage of 11 kV for short and long time scales, respectively. Both voltage

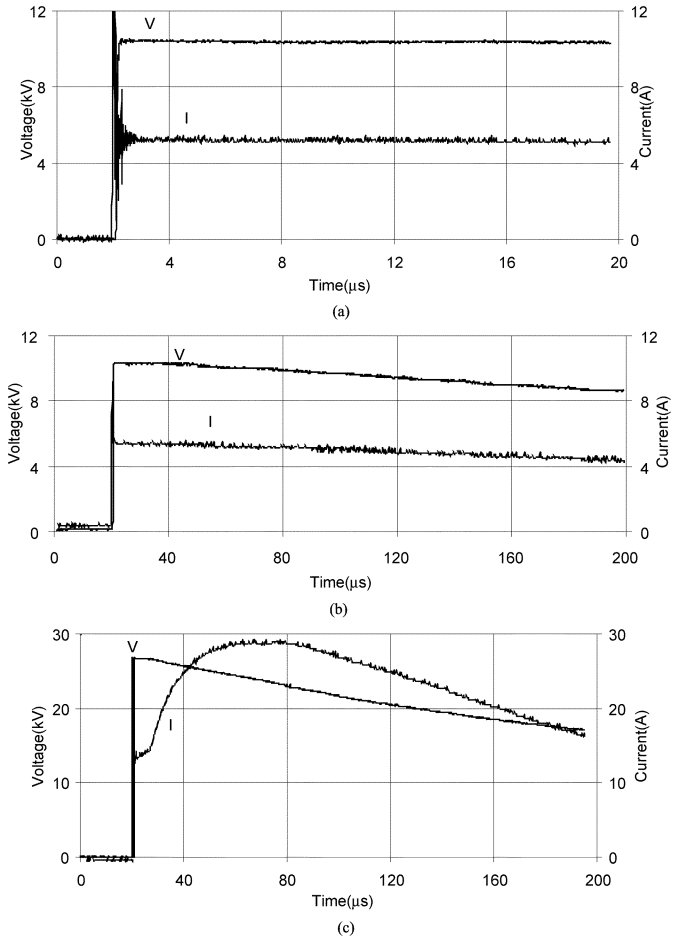

Fig. 5. Voltage and current records for sand with 3% water content. a) Linear conduction at charging voltage of 11 kV (short time scale). b) Linear conduction at charging voltage of 11 kV (long time scale). c) Nonlinear conduction at charging voltage of 27 kV.

and current traces have fast rise times. However, some initial oscillations were observed on the current trace [see Fig. 5(a)]. These initial oscillations are thought to be caused by the capacitive effects of small air spaces between the sand grains and at the interface between the soil particles and the earth electrodes. These capacitive effects were negligible when a resistive solution was used as a test medium, as can be seen in Fig. 4. When captured with a longer time scale of 20 μs/div, the voltage and current signals were found to be decreasing at a slower rate [see Fig. 5(b)] due to the relatively large value of the resistance, causing the system to discharge more slowly. As can be seen, at these low-conduction levels, the current appears to have a similar impulse shape with the voltage trace on both front and decay times, which indicates a predominantly linear resistive behavior.

For higher voltages, fast voltage and current rise times were observed. However, above a threshold level, the current impulse shape exhibited a second peak while the voltage shape continued to decrease smoothly [see Fig. 5(c)].

B. Ionization Threshold (Critical Electric Field E_c)

The critical field magnitude E_c above which soil ionization takes place is defined for the applied voltage level when the discharge current first exhibits its second peak.

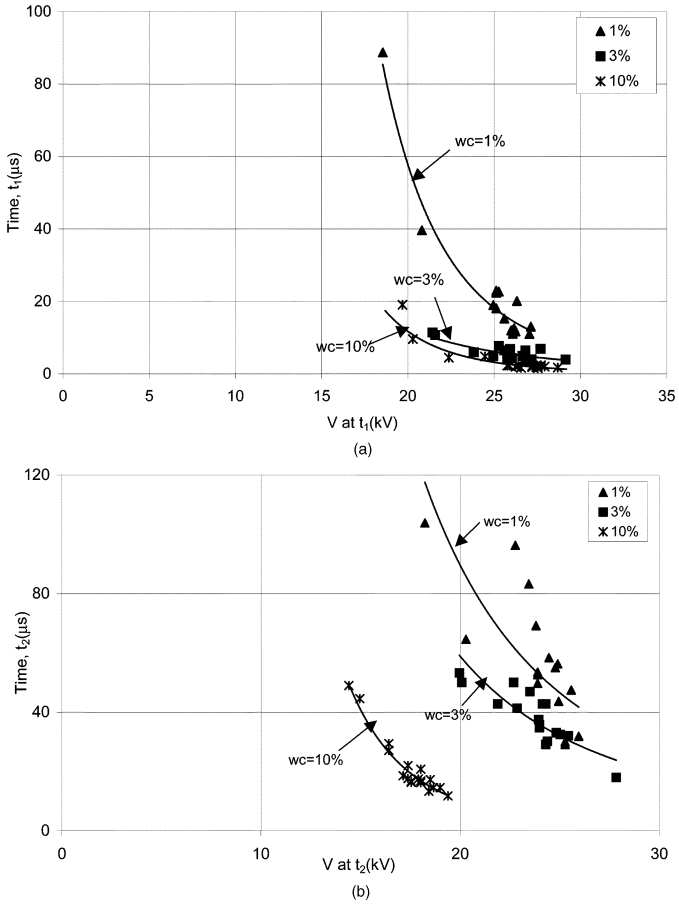

Fig. 6. Soil ionization time parameters against instantaneous voltage for sand with 1%, 3%, and 10% water content. a) Time to initiation of second current peak t_1. b) Time to second current peak t_2.

A number of methods have been suggested [6], [8], [9] to estimate E_c. In this study, it was assumed that the second current peak was caused by soil ionization. The voltage level at which this nonlinearity starts to appear was taken as the threshold voltage of soil ionization from which the critical electric field was derived.

Careful examination of the measured voltage and current traces revealed that the nonlinear soil behavior started to occur for applied voltages above 15 kV for various water contents of the sand. This voltage level shows the start of the ionization process in wet sand. Using (1), this threshold voltage produces a critical electric field E_c of 5.5 kV/cm at the surface of the energized electrode.

C. Measurement of the Soil Ionization Parameters

It is now well accepted that the second current peak [shown in Fig. 5(c)] is caused by soil ionization. As can be seen, the second current peak occurred after some time delay. From voltage and current shapes of wet sand under high currents, the time to initiation of the second current peak t_1 and time to second current peak t_2 were estimated.

Fig. 6(a) and (b) show the times t_1 and t_2 for sand with different water content and voltage magnitudes. Both time delays were found to be lower for higher conductivity soil and also to decrease with voltage magnitudes. Similar trends were observed

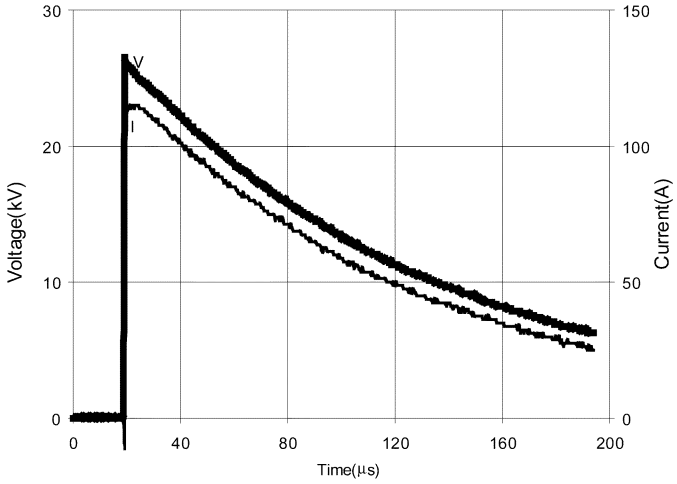

Fig. 7. Voltage and current traces for highly saturated sand (15% of water content and charging voltage of 27 kV).

when both t_1 and t_2 were plotted against current magnitudes. The results are similar to the findings obtained by Snowden and Erler [12]. These are thought to be related to the rate of propagation of the ionization process in the soil. It is likely that at low voltages and for low soil conductivity, smaller ionization regions would be produced. Thus, a slower rate of conduction growth was produced compared with that of high voltage. However, repeated tests revealed that t_1 and t_2 were distributed due to uncontrolled effects and, hence, should be described statistically. This could be due to a nonuniform water settling process, drying and heating in wet sand, and of course, the statistical nature of air breakdown.

In highly water-saturated sand, however, it is important to note that the two current peaks were not observed, i.e., sand mixed with 15% or more of water (see Fig. 7). This could be attributed to the high conductivity of the test medium. In highly wetted sand, it is possible that no ionization process occurs in this test sample for the relatively low current magnitudes used in the test since the gaps between the sand grains are filled with water. Hence, a large amount of energy is required to vaporize the water and cause localized dry zones. In addition, little field enhancement is expected to occur since there is only a small dielectric difference between the wet soil and the air voids that are now filled with water. Fast rise voltage and current traces were also observed in this highly water-saturated sand soil medium.

The initial oscillations on the current trace, as observed in sand mixed with 1%–10% of water [shown in Fig. 5(a)], were found to be negligible for sand mixed with 15% of water. This is also explained by the high resistive current that dominates in this high conductivity medium. This resistive property is also exhibited by the current and voltage traces having similar impulse shapes.

D. Pre-Ionization and Post-Ionization Impulse Resistances

The existence of the second current peak allowed the definition of two resistances referred to as [5] 1) the pre-ionization resistance (R_1) and 2) the post-ionization resistance (R_2). These resistance values were measured using the two peak currents and their corresponding instantaneous voltages. This resistance

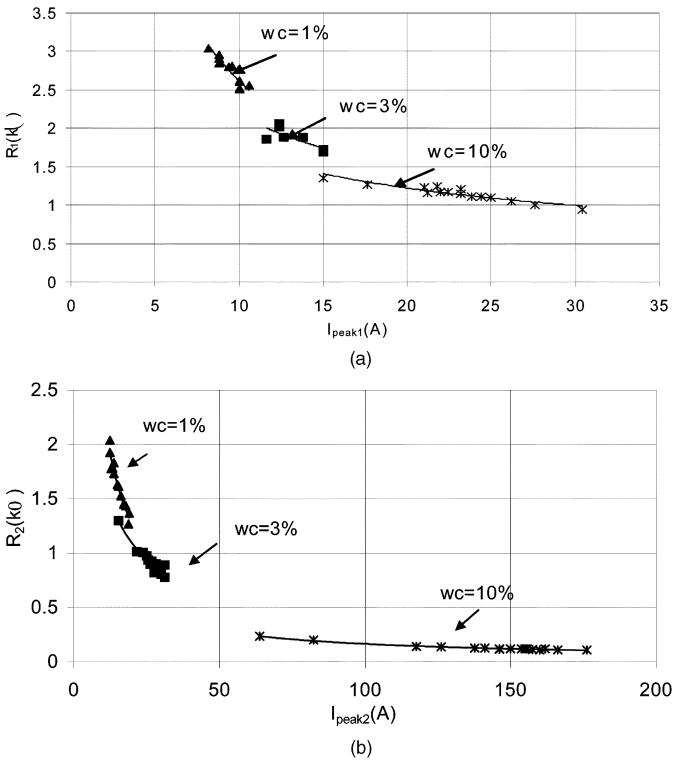

Fig. 8. Pre- and post-ionization resistances versus current peak. a) Pre-ionization resistance R_1 versus current peak. b) Post-ionization resistance R_2 (kΩ) versus current peak (A).

measurement is selected so that to eliminate any inductive effect in the test sample since at the instant of peak current $di/dt = 0$.

They are expressed as follows:

$$R_1 = \frac{V(\text{ at } I_{\text{peak1}})}{I_{\text{peak1}}} \tag{3}$$

and

$$R_2 = \frac{V(\text{ at } I_{\text{peak2}})}{I_{\text{peak2}}}. \tag{4}$$

1) Pre-Ionization Resistance: It corresponds to the soil properties without the added effect of soil ionization. It reflects the nonlinear conduction behavior governed by thermal effects and the soil structure. Graphs of R_1 were obtained for increasing applied voltage magnitudes up to the breakdown voltage of the test cell.

Fig. 8(a) shows the pre-ionization resistance R_1 obtained for sand with different water contents. It can be seen that R_1 is decreasing with current magnitudes. The decrease in R_1 with current magnitudes indicates a possible nonlinear conduction process in the wet sand resulting from thermal effects. Due to I^2R heating, the temperature of the soil increases, which will increase the conductivity and reduce the resistivity of the soil.

However, when the tests were repeated under the same impulse conditions, by replacing the test sample with a new test medium of the same sand grain size and resistivity, differences in R_1 trends were observed. This could be attributed to 1) the mechanism controlling the heating process in wet sand, which is affected by the number of shots applied to the test soil, 2) the uncontrollable water movements in wet sand, and 3) different water settling processes.

In some tests, R_1 was found to increase with current magnitude. If excessive heating in soil occurs, water vaporization in soil usually takes place. This reduces the conductivity, and, hence, increases the resistivity of the soil, thus increasing the resistance instead of reducing it as the current magnitude is increased. This excessive heating of the test soil could be minimized by limiting the number of impulse shots.

These measured variable trends of R_1 during repeated tests are in agreement with the assumption that R_1 is mainly governed by thermal conduction processes, as suggested by previous findings [12], [13]. The investigation of heating and water vaporization processes occurring in wet soil under high impulse currents, however, requires a careful temperature measurement throughout the tests. In this paper, the percentage of water content was measured after each test using a "speedy moisture meter" whose measurement is based on the pressure that is released when wet sand is reactively mixed with a reagent (calcium carbide). Only a small difference in percentage of water content was observed after the tests.

2) Post-Ionization Resistance: It corresponds to the final state of conduction that the soil reaches after the ionization region has expanded to its maximum volume within the test soil. This resistance is always lower than the pre-ionization resistance R_1.

The post-ionization resistance R_2 also decreases with increasing current magnitude [see Fig. 8(b)], and this reduction of R_2 is more significant in sand with a lower percentage of water content (high resistivity soil). As can be seen in Fig. 8(b), only a small reduction of R_2 is observed for sand mixed with 10% of water content; a range of $\sim 100\ \Omega$ to $250\ \Omega$ in the current range used in these experiments.

The resistance R_2 is governed by the ionization process that expands away from the energized electrode, thus virtually increasing the effective radius of the energized electrode and, consequently, reducing the resistance. Since this process is highly dependent on the sand characteristics and the applied voltage, the ionization process is expected to have better repeatability compared with the thermal process. When impulse tests on each sand mixture were repeated, by using a new sand sample of the same grain size and resistivity and under the same conditions, a good repeatability was observed, and very close values of R_2 were measured for similar test conditions.

E. Ionization and Drying Rates in Soil

The laboratory tests showed that sand with 1% water has the highest rate of change of R_2 with current that can be interpreted that it has higher ionization effect compared with other test samples. When the water content is small, the vaporization process produces dry regions at relatively low energies of the applied impulse. The formation of these "dry bands" allows field enhancement to occur in the band and even higher field in the air pockets within the dry soil. Such a process is expected to encourage ionization. Fig. 9(a)–(c) illustrate the effect of "dry-banding" and accompanying soil ionization, showing the resistances R_1 and R_2 as functions of peak voltage.

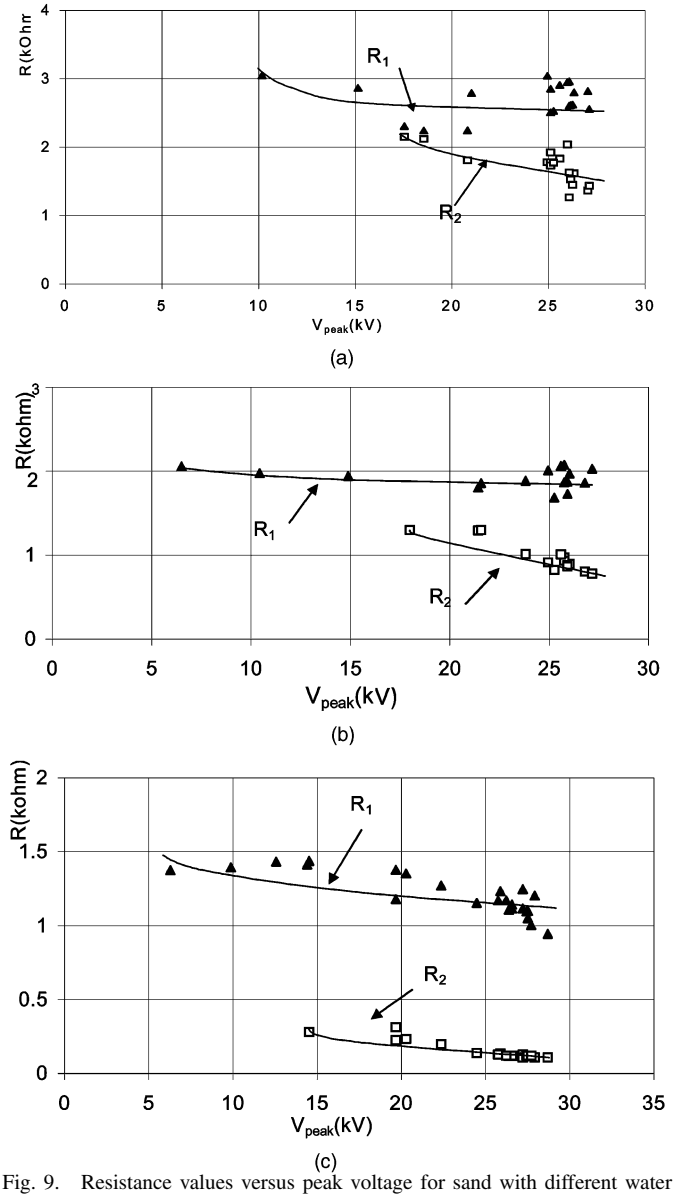

Fig. 9. Resistance values versus peak voltage for sand with different water contents. a) Sand with 1% water. b) Sand with 3% water. c) Sand with 10% water.

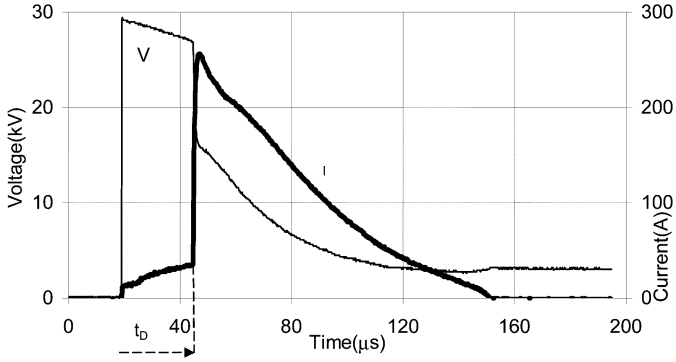

Fig. 10. Voltage and current traces when breakdown occurred in sand with 3% water content (charging voltage of 29 kV).

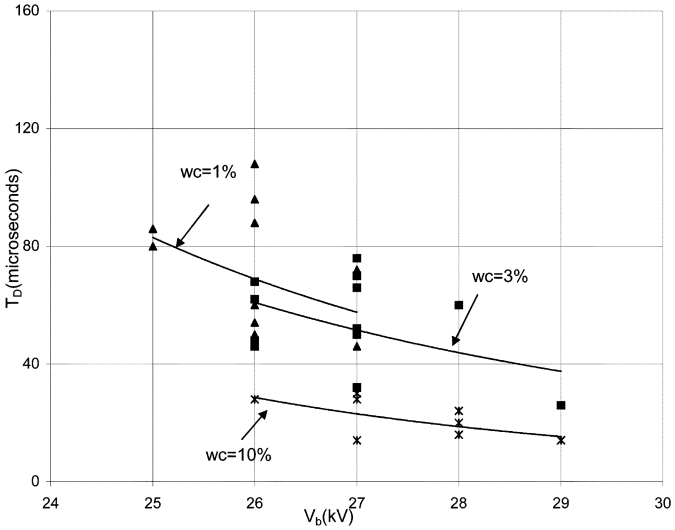

Fig. 11. Time to breakdown versus breakdown voltage for sand with three different water contents (1%, 3%, and 10% water content).

F. Soil Breakdown

1) Breakdown Parameters: In investigating the characteristics of soil ionization and measuring the magnitude of the post-ionization resistance, the charging voltage of the impulse generator was increased in small steps. After a certain voltage level, full breakdown between the energized electrode and the outer test cell container occurs through the test soil. This was observed on the voltage and current records, in which at a certain time t_D closer to the second current peak, a sudden large increase in current was accompanied by a fall to zero in voltage, indicating the instant of breakdown. Typical voltage and current traces obtained during breakdown are shown in Fig. 10. Close examination of the current impulse shape reveals an initial peak corresponding to R_1, which is followed by a second rise to the second peak current that corresponds to R_2, and it is at this second current peak that breakdown occurred.

A few holes were observed when the live electrode was carefully removed after breakdown. It was found that the number of holes is about the same as the number of breakdowns occurring in the sand.

The time to breakdown t_D is measured from a virtual origin according to IEC 60-1 [14] and is shown plotted against breakdown voltage in Fig. 11 for sand with three different percentages of water contents (1%, 3%, and 10% water contents).

The time t_D was found to be mainly dependent on voltages and conductivity of the sand. This finding is similar to the result obtained by Cabrera *et al.* [11] who found that t_D increases with increasing sand resistivity and decreases with breakdown voltage. It should be noted, however, that for some impulse shots, it was found that t_D was statistical in nature, which may be further affected by the uncontrollable water settling process and the statistical nature of air breakdown.

2) Limits of Cell Breakdown: With the assumption that the ionization process in the soil forms hemispherical shells expanding away from and increasing the size of the energized electrode, the electric field E_i at the surface of this ionization shell of radius "r_i" is determined from [16]

$$E_i = \frac{V}{r_i^2\left(\frac{1}{r_i} - \frac{1}{r_2}\right)} \tag{5}$$

with r_2 being the radius of the test cell container.

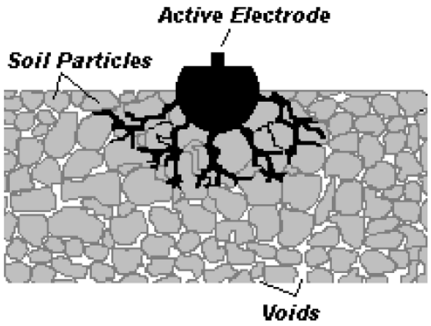

Fig. 12. Ionization propagation model.

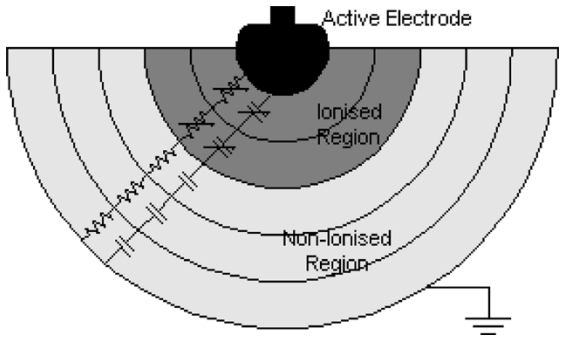

Fig. 13. Schematic of test cell with ionization regions.

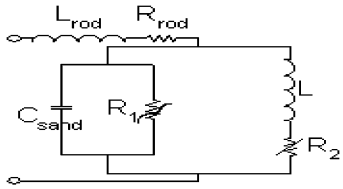

Fig. 14. Proposed equivalent circuit of soil with ionization.

We have shown [16] that the ionization expansion will continue until a critical radius r_c beyond which the field is always higher that the critical field and, consequently, breakdown will occur. This radius was found to be $r_c = r_2/2$ for the hemispherical test cell. In practice, however, small discrepancies are expected, due to the complex shape of the ionization regions and the local changes in soil physical properties.

V. Modeling of the Ionization Effect

It is now well accepted that field enhancement in voids enclosed within the soil is responsible for the initiation of the ionization process in soils. Field enhancement is caused by irregular shapes of soil grains/particles and a large difference between soil and air voids' dielectric properties. This will increase the electric field inside the air voids, and under high enough field, the air voids will be ionized. The ionization zone will increase in the form of several streamers that propagate away from the energized electrode, as illustrated in [5], shown in Fig. 12. The speed of propagation and the final length of these streamers are closely dependent on the applied voltage and soil conductivity. Assuming that the ionization regions expand uniformly with a time constant τ_i and follow the equipotential distribution in a shell form away from the energized electrode, the resistance of these shells will fall from high to low values when they become fully ionized. The dynamics of such a conduction mechanism can be described by the following expression:

$$R(t) = R_1(i)\left(\frac{R_2(i)}{R_1(i)} + e^{-(t/\tau_i)}\right) \tag{6}$$

with

R_1 pre-ionization resistance;
R_2 post-ionization resistance;
τ_i time constant for ionization propagation.

Taking into account the measured voltage and current traces on long time scales, the de-ionization process (i.e., recovery of the soil medium) appears to be happening at a slower rate (τ_{di}) than the ionization phase. This requires further experimental studies in order to quantify the rate more accurately. For this reason, an equivalent circuit approach is adopted in which the experimental data obtained for the two resistances were used.

VI. Proposed Equivalent Circuit

Since the first reported study of nonlinear soil behavior under high currents [11], much research work has been directed toward soil characterization under high-magnitude impulse currents. This also included the investigations on soil characteristics using computer models and equivalent circuit representations. In this paper, a new equivalent circuit representation that adequately simulates the observed test results is proposed.

Fig. 13 shows the test cell model and its equivalent electrical components based on the assumption of ionized regions, as discussed above. As can be seen, initially, the soil is represented by elemental parallel resistances (determined from the soil resistivity and dimensions of the elements) proportional to R_1 and capacitances determined by the soil permittivity. The ionization region is represented by much lower resistances decaying to zero in the ideal simulation. As the ionization zone increases in size, the overall resistance of the test soil will decrease accordingly (proportional to R_2). This concept lead to the formulation of an equivalent circuit, as shown in Fig. 14, which contains two main parallel branches: 1) to simulate the pre-ionization condition and 2) accounting for the ionization effects stage, including its propagation delay constant. These two branches are represented by a parallel resistance-capacitance network, with the resistance branch having a strong nonlinear voltage-current characteristic. Evidence from laboratory tests show that at very low-magnitude currents, soil behavior is affected by the capacitive effects, as can be inferred from the initial oscillations on the current signals [see Fig. 5(a)]. However, during the ionization process, the resistive current dominates, and the capacitance does not play a major role [as can be seen in Fig. 5(c)]. The expressions for the pre-ionization resistance R_1 and post-ionization resistance R_2 were derived using a curve fitting method from Fig. 6(a) and (b), respectively, for sand with different percentages of water content. Table I summarizes the empirical expressions derived for the resistances R_1 and R_2 of wet sand tested in this paper.

The laboratory test set-up together with the proposed new equivalent circuit (see Fig. 15) were simulated using the PSPICE circuit transient analysis program. In addition to this basic rep-

TABLE I
DERIVED RELATIONSHIP BETWEEN THE RESISTANCES R_1 AND R_2 AND THE CURRENT FOR WET SANDS

Sand with Water content (%)	Resistance expressions	
	$R_1(k\Omega)$	$R_2(k\Omega)$
1	$16.9.\ I^{-0.811}$	$17.61.\ I^{-0.878}$
3	$7.74.\ I^{-0.551}$	$7.63.\ I^{-0.65}$
5	$3.81.\ I^{-0.383}$	$8.69.\ I^{-0.737}$
7	$7.55.\ I^{-0.766}$	$12.33.\ I^{-0.876}$
10	$5.492.\ I^{-0.502}$	$6.323.\ I^{-0.791}$

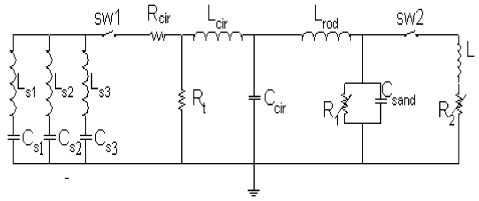

Fig. 15. Proposed equivalent circuit. $Cs1 = Cs2 = Cs3 = 0.15\ \mu$F, $Ls1 = Ls2 = Ls3 = 0.04\ \mu$H, Rcir $= 0.01\ \Omega$, Lcir $= 0.35\ \mu$H, Ccir $= 20$ pF, Lrod $= 0.1\ \mu$H, $L = 7$ mH.

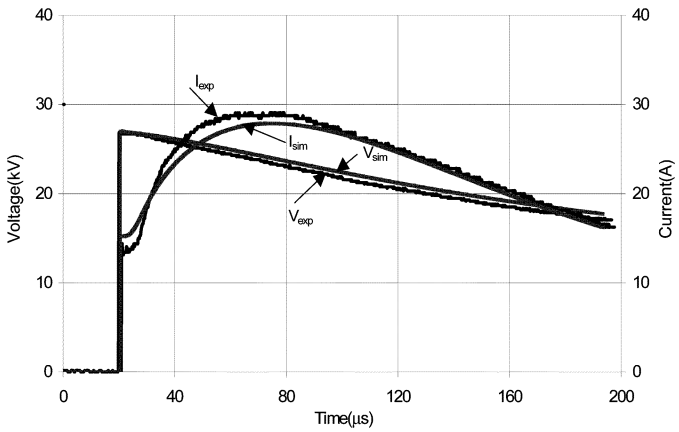

Fig. 16. Computed and measured voltage and current traces for a charging voltage of 27 kV.

resentation, other components, such as the inductive elements to represent the equivalent inductance of the test rod and simulation of the ionization delay, were also included in the simulation circuit of Fig. 15. Switch SW1 represents the impulse generator spark gap switch, and SW2 is used to initiate the ionization process, which will simulate the threshold conditions and account for the ionization time delay t_1 using an inductance element L.

Fig. 16 shows the simulated and measured voltage and current traces for a charging voltage of 27 kV and sand with 3% water content. As can be seen, the proposed equivalent circuit model can reproduce the measured nonlinearities in the impulse current shape. The simulated voltage and current traces are found to be in good agreement with measured values at other charging voltages. Using this simulation, it was confirmed that the parallel capacitance $C_{\rm sand}$ had no effect on the simulated characteristics of soil under high-impulse current magnitudes.

VII. CONCLUSION

A laboratory earth electrode test set-up was used to investigate the nonlinear conduction process occurring in sand with different water contents. An average value of breakdown voltage through the test sample was measured as 25.5 kV. This breakdown voltage was found to be independent of the percentage of water content inside the sand.

When impulse tests were conducted on a resistive solution, the resistance was found, as expected, to be constant with increasing currents. However, when wet sand was subjected to fast current impulses, its resistance decreased with increasing current magnitudes. This is due to two separate conduction phases as the current magnitude was increased. First, thermal effects due to current flow reduce the resistance; then, above the ionization threshold, the resistance is further reduced with a time constant due to expanding ionization regions. The threshold voltage for this ionization process was found to occur at an applied voltage of 15 kV, which corresponds to an electric field E_c at the energized electrode of 5.5 kV/cm. This threshold electric field was found independent of water content.

Analysis of the test data revealed a second current peak when ionization takes place in the soil. The two current peaks were used as the basis for the proposal of two new parameters of soil characteristics under high-magnitude fast impulse conditions. These are the pre-ionization and post-ionization resistances R_1 and R_2, respectively.

The effects of applied voltage magnitude and soil type on these resistances were quantified. In addition, the thermal effects were investigated, and two main processes were suggested: a) increase of ionic conduction and b) vaporization and dry banding. Other characteristics of soil ionization, such as rate of propagation and time delays, were also studied and incorporated in the formulation of an equivalent circuit.

A proposed new equivalent circuit based on the measured data was shown to reproduce the measured nonlinear current and voltage impulse shapes satisfactorily.

REFERENCES

[1] *"Earthing," British Standard Code of Practice*, BS 7430:1998.
[2] *IEEE Guide for Measuring Earth Resistivity, Ground Impedance, and Earth Surface Potentials of a Ground System*, ANSI/IEEE Std 81:1983.
[3] *IEEE Recommended Practice for Grounding Industrial and Commercial Power Systems*, ANSI/IEEE Std 142:1991.
[4] *IEEE Guide for Safety in AC Substation Grounding*, ANSI/IEEE Std 80:2000.
[5] N. M. Nor, S. Srisakot, H. Griffiths, and A. Haddad, "Characterization of soil ionization under fast impulses," in *Proc. Int. Conf. Lightning Protection*, Rhodes, Greece, Sep. 2000, pp. 417–422.
[6] A. C. Liew and M. Darveniza, "Dynamic model of impulse characteristics of concentrated earths," *Proc. Inst. Elect. Eng.*, vol. 121, no. 2, pp. 123–135, Feb. 1974.
[7] R. Kosztaluk, M. Loboda, and D. Mukhedkar, "Experimental study of transient ground impedances," *IEEE Trans. Power App. Syst.*, vol. PAS-100, no. 11, pp. 4653–4660, Nov. 1981.
[8] K. Berger, "The behavior of earth connections under high intensity impulse currents," in *Proc. CIGRE*, vol. 95, 1946.
[9] G. M. Petropoulos, "The high-voltage characteristics of earth resistances," *J. Inst. Elect. Eng.*, pt. Part II, vol. 95, pp. 172–174, Feb. 1948.
[10] V. M. Cabrera, M. S. Lundquist, and V. Cooray, "On the physical properties of discharges in sand under lightning impulses," *J. Electrostat.*, vol. 30, no. 40, pp. 17–28, May 1993.
[11] H. M. Towne, "Impulse characteristics of driven grounds," *Gen. Elect. Rev.*, vol. 31, no. 11, pp. 605–609, Nov. 1928.

[12] D. P. Snowden and J. W. Erler, "Initiation of electrical breakdown of soil by water vaporization," *IEEE Trans. Nucl. Sci.*, vol. 30, no. 6, pp. 4568–4571, Dec. 1983.
[13] V. A. J. van Lint and J. W. Erler, "Electric breakdown of earth in coaxial geometry," *IEEE Trans. Nucl. Sci.*, vol. NS-29, no. 6, pp. 1891–1896, Dec. 1982.
[14] *Guide on High-Voltage Testing Techniques*, IEC-60-1:1989.
[15] A. Haddad, P. Naylor, I. A. Metwally, D. M. German, and R. T. Waters, "An improved noninductive impulse voltage measurement technique for ZnO surge arresters," *IEEE Trans. Power Del.*, vol. 10, no. 2, pp. 778–783, Apr. 1995.
[16] S. Srisakot, N. M. Nor, H. Griffiths, and A. Haddad, "Soil ionization under fast impulse," in *Proc. Int. Conf. Gas Discharges Applications*, vol. 1, Liverpool, U.K., 2002, pp. 307–310.
[17] V. Z. Annenkov, "Sparking zones and soil breakdown with lightning current spreading out from a solid earthing conductor," *Elect. Technol.*, no. 3, pp. 53–57, 1995.
[18] A. C. Liew and M. Darveniza, "Dynamic model of impulse characteristics of concentrated earths," *Proc. Inst. Elect. Eng.*, vol. 121, no. 2, pp. 123–135, Feb. 1974.
[19] *IEEE Standard Techniques for High-Voltage Testing*, IEEE Std 4-1995.

N. Mohamad Nor, photograph and biography not available at time of publication.

A. Haddad, photograph and biography not available at time of publication.

H. Griffiths, photograph and biography not available at time of publication.